Proceedings of ASME Turbo Expo 2024
Turbomachinery Technical Conference and Exposition
GT2024
June 24-28, 2024, London, United Kingdom

GT2024-129190

CENTRIFUGAL COMPRESSOR PERFORMANCE AND FLOW PATH GENERATION WITH ARTIFICIAL INTELLIGENCE

Valentyn Barannik
SoftInWay Switzerland GmbH
Zug, Switzerland

Maksym Burlaka
SoftInWay, Inc.
Burlington, MA

Bohdan Lysianskyi
SoftInWay Switzerland GmbH
Zug, Switzerland

Leonid Moroz
SoftInWay, Inc.
Burlington, MA

ABSTRACT

Centrifugal compressors are widely used turbomachines employed across various fields as components of systems, such as being part of a turbocharger in an internal combustion engine or a refrigeration cycle. As a result of system analysis, the compressor parameters are determined with 0D or 1D solvers. Simultaneously, the compressor performance, as well as other components, influence the results of system analysis. The system analysis starts with compressor performance assumptions that could be taken from a prototype or based on the engineer's experience and prior domain knowledge. If the new design deviates significantly from the prototype, its performance assumptions diverge from the actual compressor performance, necessitating numerous iterations to align system and component parameters with overall system requirements and constraints. Therefore, the design and development projects of modern centrifugal compressors are lengthy and very expensive.

The research described in this paper aims to develop highly accurate single-stage centrifugal compressor performance models coupled with flow path geometry generation models leveraging artificial intelligence (AI) technology. These models offer the potential to circumvent expensive design-build-test iterations, thereby substantially reducing the time and cost of developing modern centrifugal compressors.

In this paper, the various configurations of centrifugal compressors are considered, along with a description of the configurations of interest. The selection of input and output variables that provide sufficient information about compressor design with the respective ranges is justified. There is a detailed description of automated workflows for centrifugal compressor design and performance data generation for neural network training. The approaches for data preprocessing that enable high-accuracy predictions are provided, and the peculiarities of applying the AI technology developed by the authors for centrifugal compressors are discussed. An analysis of the trained model accuracy as well as the technique for quantitative assessment of prediction reliability is provided. The utilization of the centrifugal compressor AI model integrated into a gas turbine engine simulation environment is demonstrated.

Keywords: Centrifugal Compressor, Flow Path, Performance Map, Machine Learning, Artificial Neural Network

NOMENCLATURE

AI	Artificial Intelligence
ML	Machine Learning
1D	One-Dimensional
2D	Two-Dimensional
3D	Three-Dimensional
CFD	Computational Fluid Dynamics
NN	Neural Network
AutoML	Automated Machine Learning
RPM	Revolutions Per Minute
MSE	Mean Squared Error
MFR	Mass Flow Rate
ptr	Total-to-Total Pressure Ratio
eff_tt	Total-to-Total Efficiency
Deqx	Equivalent Diffusion Factor
ReLU	Rectified Linear Unit
D1t	inlet tip diameter
D1h	inlet hub diameter
D2	outlet diameter
z	number of blades
B	axial length of the compressor wheel
lc2	outlet impeller blade height
FFNN	Feed Forward Neural Network
SVM	Support Vector Machine
GBPNN	Gaussian kernel function back propagation neural network
IGV	Inlet Guide Vane
GTU	Gas Turbine Unit
AE	Autoencoder

1. INTRODUCTION

In the process of conducting a system cycle simulation, engineers should define the realistic performance levels expected from the components to be employed. These performance metrics can be established through past experiences or based on empirical correlations [1]. After that, the first iteration of the cycle simulation is executed. Once the boundary conditions are computed, they are then handed over to a design engineer for the preliminary design of the component based on different fidelity levels (1D/2D/3D) [2, 3]. This involves determining both the dimensions and the component performance. However, the determined performance may significantly deviate from what was initially assigned. That leads to the necessity of performing additional iterations between cycle simulation and preliminary design levels, which elongates the duration and increases the costs of the project.

There is an opportunity to minimize the number of iterations between the system analysis and preliminary design phases. This can be achieved by improving the performance estimation accuracy, coupled with the flow path geometry prediction procedure for different compressor configurations, accounting for off-design modes and avoiding the need to pass the compressor design task to the compressor team during the system analysis step.

This study involved the development of an approach for estimating the performance and dimensions of centrifugal compressors with a fidelity comparable to 2D streamline results, significantly reducing time compared to existing 2D approaches. The developed approach is intended for use at the cycle simulation level, enabling engineers to quickly identify the optimal compressor design while considering design restrictions.

As mentioned above, compressor performance estimation can be solved using the numerous codes that are currently available. The fidelity of these codes varies from 1D to 3D CFD. 1D provides the results with a relatively brief time range, but it is based on empirical correlations or analytical equations derived with certain assumptions only valid in limited ranges [4]. The modern requirements for compressors demand higher fidelity and more assuredness in predictions. For higher fidelity, 3D CFD codes are used [5, 6]. They are more universal in this respect, but they are much more resource-intensive compared to 1D.

The employment of autonomous ML technologies allows for the obtainment of the speed of performance prediction faster than 1D codes and the fidelity comparable to 3D CFD codes if 3D CFD results are contained in the training data set.

ML technologies are successfully used in areas of visual recognition, natural language processing, evidence-based treatment plans, games, and many others. However, despite remarkable success in the areas mentioned above, the application of AI for the prediction of compressor performance is just starting to be widely considered. The authors of [7] compared loss-analysis-based model prediction results with the Kriging model and neural network model. The results show a higher accuracy in interpolation and extrapolation capabilities of loss-analysis-based models in comparison with other models. However, the study was performed for a single performance map only, and there is no comparison of the used model's prediction for different compressor geometries and different shapes of speedlines. The authors do not address the question of selecting the optimal neural network architecture, which could influence the predicting capabilities of the neural network. Gholamrezaei and Ghorbanian [8] used FFNN for the generation of the performance map of axial compressors, employing the experimental data. The architecture of FFNN was selected based on empirical investigation that may not be optimal. The study is performed for a single performance map. Fei and Zhao [9] applied GBPNN and compared it with FFNN and SVM methods to check their interpolation and extrapolation capabilities for axial compressor maps. In [10] authors used SVM with a genetic algorithm to optimize its parameters to predict the performance of a compressor under all operating conditions through limited data. Loryś and Orkisz [11] checked the interpolation and extrapolation capabilities of FFNN accounting for the "relative stability margin" in the training process. In [12] authors applied FFNN to predict compressor characteristics of a single spool turboprop engine. Massoudi and others [13] used neural networks to generate fast and accurate high-fidelity models for small-scale turbocompressors. The optimization task based on the genetic algorithm was formulated to determine the optimal set of network hyperparameters. The trained AI model is then used to determine the optimal robust design of the compressor.

Despite there being many publications that consider the application of NN for compressor performance prediction, most of them cover a single performance map and analyze interpolation and extrapolation capabilities in comparison with other approaches. That approach does not completely open the capabilities of NNs to predict compressor performance for different designs and layouts. Moreover, the architecture of NNs used in publications is not optimal and selected based on empirical or author assumptions, which could significantly influence prediction results.

This work was focused on advancing the application of ML technologies for centrifugal compressor performance predictions accounting for different configurations and consists of three major steps:

1. Adopt the procedure outlined in [14] for creating an AI-based model used for performance prediction of the centrifugal compressor.
2. Develop the algorithm and train the AI model for centrifugal compressor geometry predictions.
3. Study the applicability of the trained AI models for centrifugal compressors in the cycle simulation tool to identify the most efficient compressor design.

2. APPROACHES AND METHODS

The following technical activities were performed:

- Centrifugal compressor design
- Training data generation and pre-processing
- ML techniques, hyperparameters fine-tuning, and training

- Utilization of the trained centrifugal compressor models along the GTU cycle simulation.

This section describes the approaches and methods used for every type of technical activity.

2.1 Compressor Design

In this work, the training data consists of the geometry generated for various configurations of single-stage centrifugal compressors and the corresponding performance for the compressor operational range. There are multiple configurations of centrifugal compressors: single stage or multistage, with IGV or without, with volute or without, etc.

The training data generated in this work consists of four configurations of a compressor: impeller with splitters and without, layout with vane diffuser after the impeller, and without a vane diffuser. All configurations include a volute.

The compressor flow path design and the performance estimation of the designed flow path were calculated using AxSTREAM® and its respective modules and solvers [2]. In particular, compressor design was performed with a Preliminary design module. The 2D streamline solver was used by employing loss model correlations based on Aungier [15]. The reliability of the compressor performance prediction utilizing the AxSTREAM® solvers is confirmed by numerous validation cases and a couple of them are provided below.

FIGURE 1 represents case 1 validation results of the 2D solver for the centrifugal compressor [16]. In turn, FIGURE 2 shows case 2 with the comparison of 2D solver results with test data from [17]. As it can be seen in the figures there is good agreement between the test data and 2D solver results, justifying the use of the solvers for generating sufficiently accurate datasets for AI training.

The design of the compressor is determined by 15 variables:

1. categorical variable that determines the splitter presence for design
2. categorical variable that determines the presence of a vane diffuser after vaneless one
3. design point pressure ratio
4. design point mass flow rate
5. flow factor
6. work coefficient
7. relative diameter ratio at the inlet
8. specific speed
9. blade loading
10. meridional velocity ratio (outlet to the inlet of the impeller)
11. impeller incidence angle
12. the axial length of the impeller
13. relative clearance
14. radial length of a vane diffuser
15. radial length of a vaneless diffuser

The radial length of the vane diffuser and the radial length of the vaneless diffuser variables depend on the layout of the compressor. If the layout does not include the vane diffuser, then the radial length of the vane diffuser is equal to zero and the radial length of the vaneless diffuser is varied in the specified ranges. Otherwise, the radial length of the vaneless diffuser is equal to 1.08 and the radial length of the vane diffuser is varied.

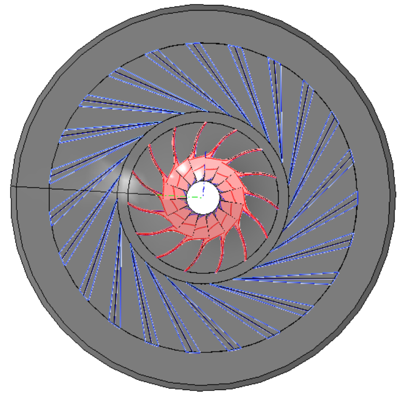

A) GEOMETRY OF COMPRESSOR [16]

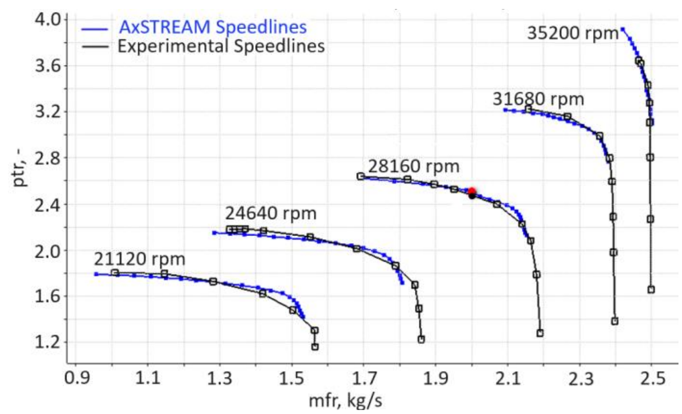

B) PRESSURE RATIO MAP FOR COMPRESSOR [16]

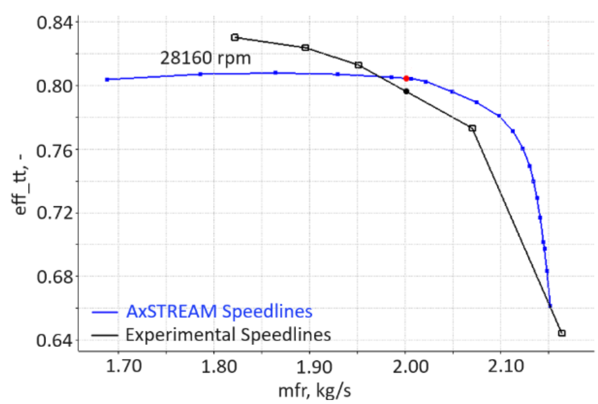

C) EFFICIENCY MAP FOR COMPRESSOR [16] AT DESIGN ROTATIONAL SPEED

FIGURE 1: CASE 1 VALIDATION OF SOLVER WITH COMPRESSOR [16]

Additionally, the off-design rotational speed and off-design mass flow rate are used to predict the performance of the compressor at off-design modes.

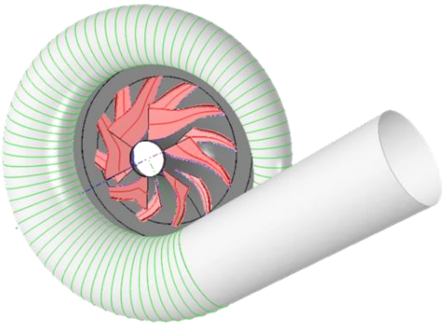

A) GEOMETRY OF COMPRESSOR [17]

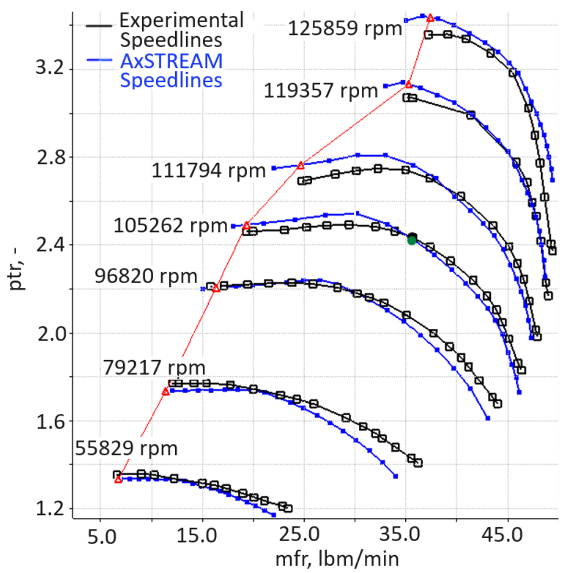

B) PRESSURE RATIO MAP FOR COMPRESSOR [17]

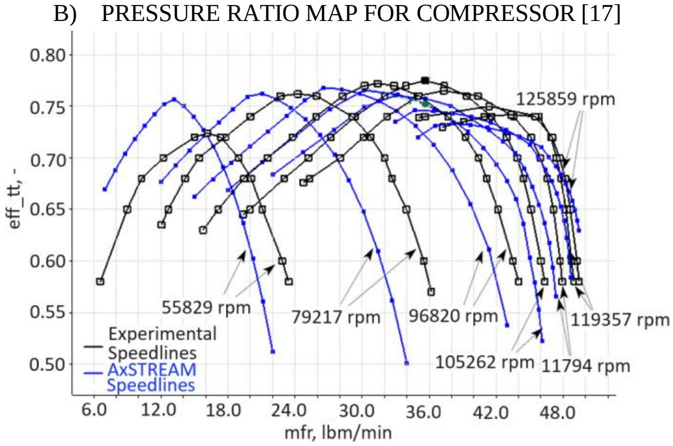

C) EFFICIENCY MAP FOR COMPRESSOR [17] AT DESIGN ROTATIONAL SPEED

FIGURE 2: CASE 2 VALIDATION OF SOLVER WITH COMPRESSOR [17]

All this data is used as the input parameters for the preliminary design. The designs were generated for fixed inlet total pressure and inlet total temperature. The working fluid is air. The design variables and constraints were selected to cover the wide range of compressors used in the automotive industry, refrigeration, aerospace, HVAC, etc.

Sobol sequence [18] is used to generate the combinations of variables.

2.2 Training Data Generation and Pre-processing

Once the combination of the design variables is generated, the data is transferred to the preliminary design procedure. In case the design cannot be generated for the combination of variables, the current action is stopped for this combination and the following combination is evaluated.

Otherwise, if the preliminary design of the flow path was completed successfully, the generated design is used for further actions.

To automate the process of training data generation, an automated workflow was developed (FIGURE 3). The first section of the workflow is responsible for the compressor design procedure and geometrical data-set generation. It should be noted that the preliminary design procedure is based on an inverse task formulation, and the results of the direct calculation of the compressor may be slightly different. To save the dataset and the results of the direct task formulation, additional actions are automatically performed before the design is saved. The design procedure includes the utilization of 3D geometry for more accurate determination of the throat area, checking if the design is close to choke, estimating 2D performance at the design mode, and adjusting the relative clearance value if, after the design procedure, the absolute clearance value is out of the physical range.

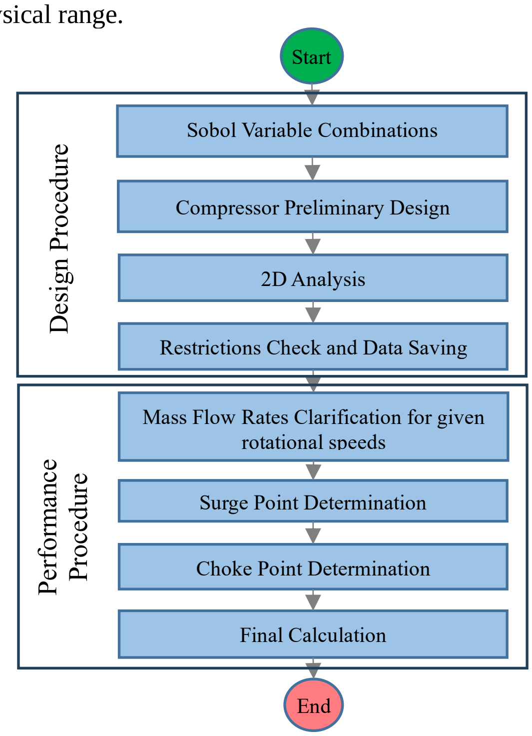

FIGURE 3: AUTOMATIC WORKFLOW FOR COMPRESSOR PERFORMANCE DATA GENERATION AND PRE-PROCESSING

In the current study, 51 geometrical parameters were extracted from each generated design and utilized as output data for AI model training. Furthermore, the designs are used to calculate the performance of compressors.

The goal of the performance estimation part of the workflow is to prepare raw data coming from the compressor performance calculation code to a form suitable for successful training, i.e., remove outliers, smooth choke, and surge limit lines, and save the data set in a proper format. In particular, surge point determination is performed based on the criteria of the maximum allowable equivalent diffusion factor value (Deqx) [15]. This factor determines the onset of flow separation on the blade surface. The choke point was determined based on the criteria of an efficiency drop by 40% relative to the maximum efficiency value on the speedline. Performance points beyond the surge and choke points were considered as outliers.

It should be noted that the workflow presented in FIGURE 3 is a schematic representation. Every block in the figure is a block scheme created in AxSTREAM ION™ where certain blocks and scripts were integrated into a specific algorithm that processes the data. For example, the workflow for the determination of surge points is shown in FIGURE 4.

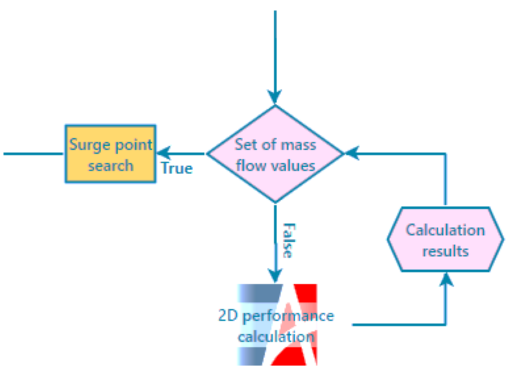

FIGURE 4: WORKFLOW FOR DETERMINATION OF SURGE POINT FOR THE SPECIFIED SPEEDLINE

In FIGURE 4 the "Set of mass flow values" iterates through the initial range of the assumed mass flow values where the speedline may theoretically exist and be determined by the "Mass Flow Rates Clarification for given rotational speeds" algorithm. Each iteration involves estimating the performance point, and the Deqx value while tracking the identifiers of the solver's successful completion, and saving the calculation results for future proceedings. Once all mass flow points have gone through the calculation, the results are transferred to the implemented methodology that determines the exact value of the mass flow, which corresponds to the required Deqx. The methodology is based on approximating the results of successful solver execution using the Catmull-Rom spline [19].

The presented workflow was successfully used to generate data sets for all considered compressors.

During the process of preparing the data sets for compressor performance model training, the authors use a parametric model-based approach for the representation of the compressor maps to improve the quality of prediction of the speedline shapes. This is because preliminary predictions of performance as separated points showed that the shape of speedlines was predicted incorrectly due to unrealistic oscillations near the surge point.

The requirement for the parametric model was flexibility sufficient to represent the wide variety of speedline shapes on one hand and inherited correspondence to the typical shape of speedlines without unrealistic oscillations on the other hand. The flexibility of polynomials of the second order was not sufficient. In turn, the polynomials of the third or higher orders suffered from unphysical fluctuations. The flexibility and fit of speedlines for centrifugal compressors with satisfying accuracy were ensured by combining three Bezier curves [20]: one linear Bezier curve and two quadratic Bezier curves in the middle section of the speedline and at the surge region. The developed parametric model (FIGURE 5) was used for representing pressure ratio and efficiency curves vs mass flow. The model was named parametric Model 2. Model 1 which was used for the parametrization of pressure ratio curves of axial compressors is described in [14]. The connections of the sections of the combined curve are tangent to each other at respective connection points P0 and P2 forming a composite Bezier curve.

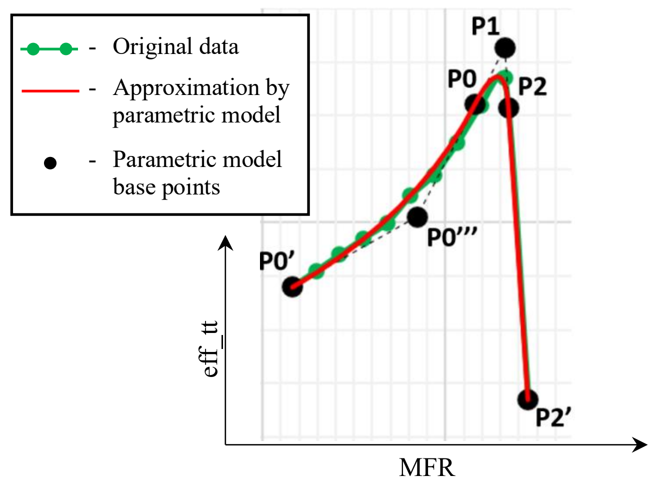

FIGURE 5: PARAMETRIC MODEL 2

The linear and quadratic Bezier curves are determined by equations (1) and (2) respectively, accounting for (3).

$$\boldsymbol{B}(t) = \boldsymbol{P}_0 + t(\boldsymbol{P}_1 - \boldsymbol{P}_0) \tag{1}$$

$$\boldsymbol{B}(t) = (1-t)[(1-t)\boldsymbol{P}_0 + t\boldsymbol{P}_1] + t[(1-t)\boldsymbol{P}_1 + t\boldsymbol{P}_2] \tag{2}$$

$$0 \leq t \leq 1 \tag{3}$$

where, t – is a parameter; and $\boldsymbol{P}_0, \boldsymbol{P}_1, \boldsymbol{P}_2$ – are Bezier curve base points in the respective coordinate system.

According to Model 2, the shape of the combined curve is fully determined by 10 parameters: two coordinates of surge point **P0’** plus two coordinates of choke point **P2’,** along with six dimensionless factors determining the relative locations of the other four base points.

The transformation of the training, validation, and test data sets to a parametric view is performed by the Levenberg-Marquardt algorithm [21].

Besides fitting the generated data, additional manipulations were conducted to prevent the emergence of unphysical shapes in the predicted speed lines. In particular, to avoid the "mirror" speedlines which are caused by the error in the prediction of mass flow rate at the surge and choke points, the substitution of surge mass flow value is performed. The resulting surge mass flow value in this case is the difference between the predicted choke mass flow rate and the predicted difference in the choke and surge point mass flow rates. As the quality assessment of the result shows, such substitution positively affects the model accuracy, especially for the speedlines where the difference between surge and surge point mass flow rates is small. The difference between choke and surge mass flow rates is always positive, so the results of the trained model prediction are also positive. Consequently, this prevents the occurrence of predicted speed lines with a surge point to the right of the choke point.

A similar approach is used for pressure ratio values, where the speed lines are almost horizontal.

2.3 ML Techniques, Hyperparameters Fine-tuning, and Training

2.3.1 Performance Prediction

Different machine learning approaches/techniques can be used to predict compressor performance, such as the Kriging model, feedforward neural networks with back-propagation, Gaussian kernel function, support vector machines, and others [7-13].

Previous studies showed that utilization of feedforward neural networks (FFNN) with back-propagation with a focus on the search for optimal hyperparameters based on AutoML approaches, provides the required accuracy of performance-trained models [14].

In [14] the AutoKeras algorithm [22] with Greedy tuner [23] is used for the search for optimal combinations of hyperparameters like the number of hidden layers, number of neurons in every layer, activation functions, learning rates, and dropout.

MSE as a loss function and the "Adam" optimizer [24] were used for regression models. The data was normalized using a standard scaler [25].

The detailed justification of AutoKeras selection among the various AutoML approaches is presented in [14]. The number of trials for performance model training is equal to 20.

It should be noted that the accuracy metric for the trained models was quantified as the percentage of speedlines that have a prediction error less than a specified threshold. The prediction error is calculated using equation (4) for every speedline from validation and test sets. The target value is 95% of all speedlines should have a relative difference < 5 % (equation (4)) in pressure ratio and efficiency.

$$RD = \frac{2\sum_{i=1}^{n}(|A_{i-1} - P_{i-1}| + |A_i - P_i|)\cdot(G_i - G_{i-1})}{\sum_{i=1}^{n}(A_{i-1} + P_{i-1} + A_i + P_i)\cdot(G_i - G_{i-1})} \qquad (4)$$

where, A_i, A_{i-1} - the actual values of the considered parameter at the current G_i and previous G_{i-1} value of mass flow rate; P_i, P_{i-1} - the predicted values of the considered parameter at the current G_i and previous G_{i-1} value of mass flow rate.

In the data sets transformed for the training of NNs to predict parametrized curves described in the previous section, the performance points belonging to a speedline are replaced with 10 parameters for pressure ratio and efficiency curves. It was determined that, unlike in [14], where the coordinates of the choke and surge points play a much more substantial role in the final level of error for speedlines compared to the dimensionless factors, in centrifugal compressor speedlines with relatively low rotation speed, the dimensionless parameters also play a substantial role in predicting accuracy. Therefore, for the current study, the training process includes not only separate NNs for every coordinate of the choke and surge point but also separate NNs for dimensionless factors of parametric curves. Such a split still allows having the common models for the prediction of Choke MFR and Surge MFR and using them for ptr and eff_tt. Moreover, it allowed consistency in MFR values across all models. All models were trained independently, and then, at the inference step, the predictions of all the models were combined to recreate the entire speedline. The total number of models for the four considered performance parameter predictions (ptr and eff_tt) consists of 34 models.

The required inputs to the model are the design parameters described in Section 2.1 and rpm and mfr at off-design. As the models predict the speedline choke and surge point locations it is also possible to use a trained model to predict the entire speedline. For this goal, the MFR definition was not obligatory.

To estimate the uncertainty level of the prediction results, additional NN models were trained with different initial guesses for the model weight coefficients. The additional model training is performed once the optimal architecture of NN is determined by the AutoKeras algorithm. In this case, the result of the NN prediction is the average value of the variable for all additional models. The uncertainty level is determined by the maximum and minimum values of the variable across all additional models. The total number of uncertainty models is 20.

2.3.2 Geometry Prediction

The architecture of the geometry prediction model consists of a combination of two NN types: autoencoder (AE) and FFNN.

Training of the models includes the following steps:

- Utilization of autoencoders to train encoder and decoder parts
- Replacing the encoder part by FFNN and training this network to preserve the decoder part

As multiple testing results show, such a network structure allows for more accurate predictions compared to a simple FFNN architecture. The difference is especially noticeable for the geometrical model that contains a large number of outputs (geometry of multistage turbomachines).

Accuracy estimation was performed using the same criterion as for performance prediction (equation 4).

It should be noted that the architecture of the NN for the geometry prediction model depends on the number of input and output variables. The utilization of AutoKeras, as it is for performance models, will be tested in future studies.

MSE was used as the metric for continual and discrete parameters. Optimization of the model for categorical parameters prediction such as splitter presence and type of layout was based on the Categorical Cross-Entropy loss function [26]. The one-hot encoding approach [27] was applied to the categorical variables. The main goal of this approach is to prevent the model's poor performance or unexpected results by avoiding a natural ordering between categories.

It should be noted that utilization of such an approach makes it impossible to train a separated model for each output variable, as they are dependent on the same latent space, and created by training autoencoder.

The uncertainty estimation of the output parameter is different from the performance prediction (FIGURE 6). Here the training process has started for the specified number of models (n) that are hyperparameters for the algorithm. The goal of NN training is to minimize the deviation between the average NN prediction and real value. The training process is then repeated k-times, which are represented as separate k branches in FIGURE 6. The result of NN prediction is the average value of all k-results predictions and the uncertainty range is the maximal and minimal value of variable for all k-results. For this study n=10 and k=10.

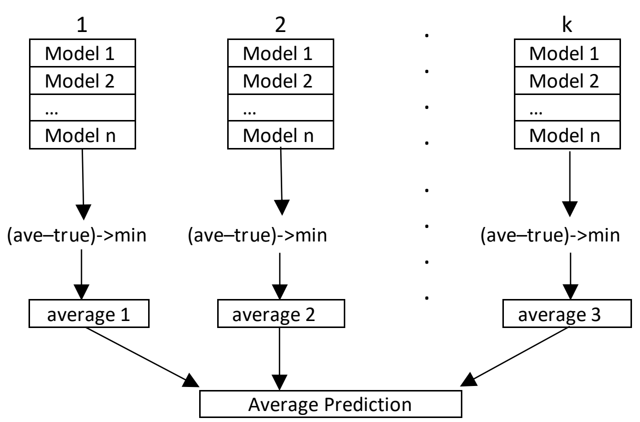

FIGURE 6: UNCERTAINTY DETERMINATION FOR GEOMETRY MODEL

FIGURE 7 shows the accuracy variation at different n and k values. As can be seen at the low n value, the accuracy for k=1 is higher than for k=10. This is because, for k=10, 20-30% of the n models have an accuracy lower than 80% which reduced the resulting model accuracy. In turn, for the case n=1 and k=1, the model with a higher accuracy is used. With the rise of n, and with the fixed k value, the influence of n "bad" models becomes lower. Further rise of n for fixed k leads to the resulting model accuracy growth. The accuracy of the resulting model is higher for higher values of k. However, for k=10 increasing the n value to higher than 9 does not lead to significant accuracy gains. Thus, taking into account that accuracy at n=10 and k=10 was almost equal to 1, the further increase of n and k was not justifiable for our case.

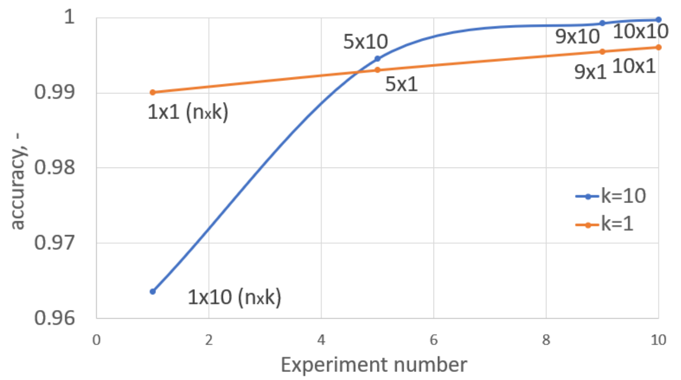

FIGURE 7: MODEL ACCURACY WITH DIFFERENT N AND K

2.4 Utilization of The Trained Models in System Simulation Environment

To analyze the possibility of determining the optimal design of a centrifugal compressor by calculating the thermodynamic cycle, the gas turbine unit (GTU) cycle was created in a system simulation environment (FIGURE 8).

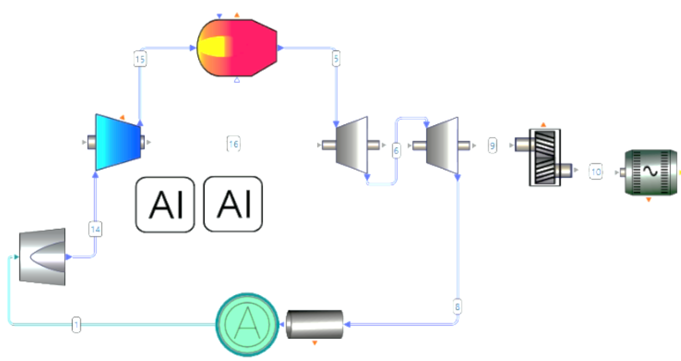

FIGURE 8: GTU CYCLE TO TEST TRAINED AI MODELS

The GTU cycle in FIGURE 8 includes the following main components: intake, compressor, gas generator, compressor turbine, power turbine, and generator. The AxSTREAM System Simulation™ tool was used to integrate the trained centrifugal AI models (geometry and performance) using API. It should be noted that the AI component for model integration is independent and can be related to any component in the system simulation tool, e.g. turbine, heat exchanger, combustor, etc.

In this study, the cycle simulation environment provides the boundary conditions to AI models and gets back the performance level and geometry values. The AI performance estimation procedure is called at each internal iteration of the system simulation solver.

The goal of the optimization is to determine the optimal combination of compressor design parameters that maximize efficiency. The Differential Evolution algorithm [28] is employed as the optimization method. The population size is 100, the number of iterations is 30, the "polish" option is set to true, and the accuracy is 1E-5.

The results of the simulation are presented in section 3.3.

3. RESULTS AND DISCUSSION

Leveraging the approaches and methods described in the previous section, the respective technical activities were performed. Selected results are presented and discussed in this section.

3.1 Training Data Generation and Pre-processing Results

Utilizing the workflow described in section 2.2, the performance and geometry data were generated for a wide range of pressure ratios and mass flows. The generated data was then pre-processed and prepared, i.e., the generated data sets were clean and ready to be used for training.

The following data sets were generated:

- Geometry: 33,498 geometry points in the training data set.
- Performance: 3,128,586 performance points in the training data set that corresponds to 14,900 compressor designs.

After transforming separated speedline points to Bezier splines representation by automatic curve fitting as described in Section 2.2, the final number of points for performance prediction consists of 104,000 points.

Examples of the generated data with automatic curve fitting for total-to-total pressure ratio (ptr) and total-to-total efficiency (eff_tt) are presented in FIGURE 9 and FIGURE 10.

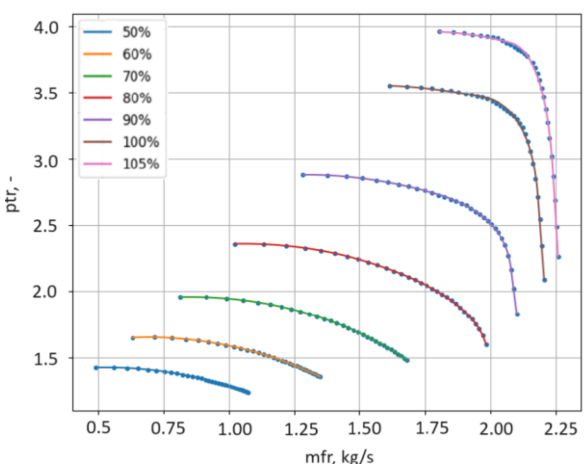

FIGURE 9: TOTAL-TO-TOTAL PRESSURE RATIO AUTOFITTING EXAMPLE

In FIGURE 9 and FIGURE 10, the dots represent the performance points from the generated data sets, and the lines are fitted curves by the parametric model described in Section 2.2. The legend represents rotational speed in % to the design speed. It can be seen that Model 2 has sufficient flexibility to approximate the wide variety of speedline shapes and does not have any unphysical oscillations or kinks. It should be noted that the presented performance curves do not contain sharp spikes. In [14 and 29] it was shown that Model 2 was able to represent even sharp spikes of efficiency curves that are typical for high-loaded axial compressors.

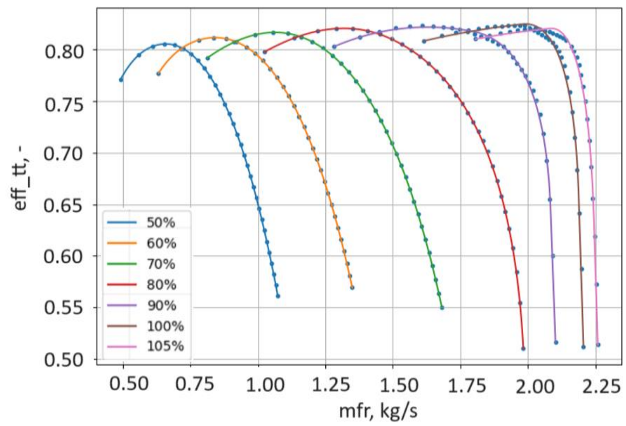

FIGURE 10: TOTAL-TO-TOTAL EFFICIENCY AUTO FITTING EXAMPLE

3.2 Training Results

3.2.1 Geometry Prediction Results

The results of geometry model training show that for 99.7% of validated designs the geometrical parameters prediction error does not exceed 5%, and the error for 99.9% of designs does not exceed 10%.

The example of the predicted geometry inserted into AxSTREAM® is shown in FIGURE 11.

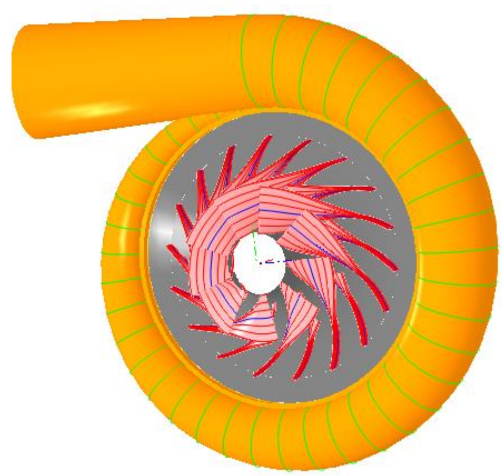

FIGURE 11: PREDICTED GEOMETRY LOADED IN AXSTREAM®

TABLE 1 demonstrates the geometrical model prediction for validated designs.

TABLE 1: PREDICTION ERRORS FOR GEOMETRY

	D1t error, %	D1h error, %	D2 error, %	z error,%	B error,%	lc2 error,%
Design1	0.23	1.10	1.10	0.00	1.52	2.46
Design2	0.07	0.15	0.15	0.00	0.20	2.64
Design3	0.06	0.02	0.02	0.00	0.03	0.14

FIGURE 12 shows the compressor performance calculated in AxSTREAM® based on the predicted geometry ("predict" line in the figure) and the performance from the validation dataset ("true" line in the figure) that was generated using the automated workflow (Section 2.2). This is to demonstrate the quality of centrifugal compressor flow path geometry predictions.

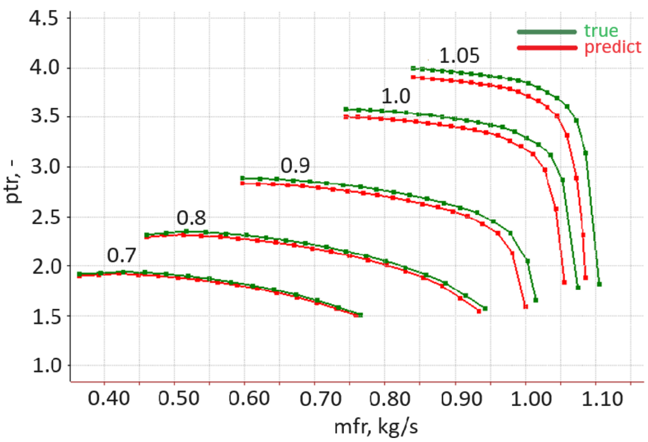

FIGURE 12: COMPRESSOR MAP FOR THE TRUE AND PREDICTED DESIGNS

It can be seen that the developed approach for geometry prediction allows getting the geometry of the centrifugal compressor with high accuracy. It was determined that the main reason for performance map deviation is the difference in the prediction of throat value. Due to this, the choke point of the restored geometry takes place at a lower mass flow rate. The ways of increasing the accuracy of throat value prediction will be investigated in further research.

3.2.2 Performance Prediction Results

The average accuracy of the performance model is 99.6% with an error threshold of 5%, and 99.9% with a 10% error threshold respectively. Wherein the higher accuracy level was reached for the ptr parameter (99.9 %). Efficiency prediction accuracy was 99.4%.

The results of ptr and eff_tt prediction with the uncertainty range for the design of the validation data set are presented in FIGURE 13 and FIGURE 14.

It can be seen that the approaches used for data preprocessing allow for the acquisition of the physical shape of speedlines. Utilization of the AutoML algorithm in combination with additional training for uncertainty level calculations provides satisfactory accuracy of predicted results. It should be noted that there are still regions of model prediction where the uncertainty level is higher and more data might needed in those regions to reduce it.

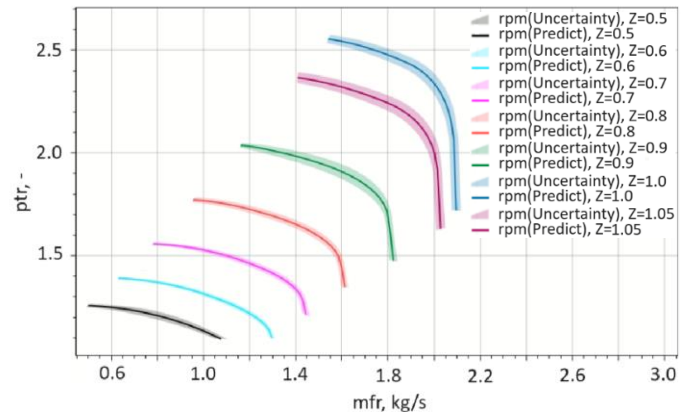

FIGURE 13: COMPRESSOR MAP (PTR) PREDICTED BY TRAINED MODEL

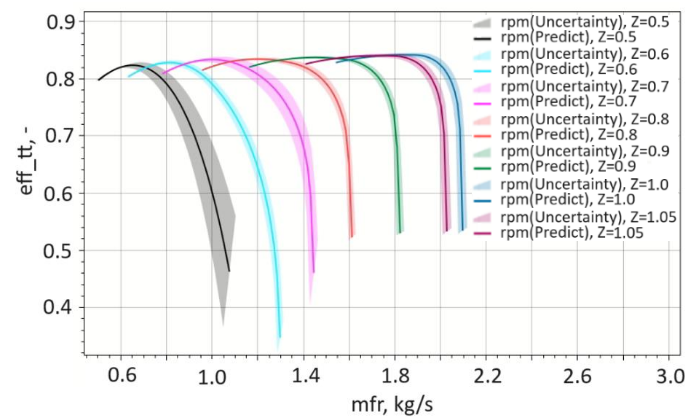

FIGURE 14: COMPRESSOR MAP (EFF_TT) PREDICTED BY TRAINED MODEL

3.3 AI Model Utilization in The Cycle Analysis Results

The cycle simulation was started with two values of mass flow, 3.8 kg/s which corresponds to the small turboprop engines, and 20 kg/s. The varied parameters are:

- splitter presence for design (splt)
- vane diffuser after vaneless one presence (layout)
- specific speed (ns)
- blade loading (BL)
- flow factor (Cz/U)
- radial length of vane diffuser (k_VD)
- radial length of the vaneless diffuser (k_VLD)

The result of the optimization is presented in TABLE 2. The table shows that the optimal solutions contain the variable values that are reasonable for centrifugal compressors. It should be noted that the values of k_VD are lower than expected for the designs with a high-pressure ratio (the pressure ratio in this case is 5). There is an assumption that such behavior of k_VD can be the reason for combining different configurations into a single model. This question will be analyzed in the future.

TABLE 2: OPTIMAL GEOMETRICAL PARAMETERS ALONG THE CYCLE SIMULATION

mfr, kg/s	splt	layout	ns	BL	Cz/U	k_VD	k_VLD	eff_tt
3.8	1	1	0.795	0.435	0.5	1.15	1.08	0.836
20	1	1	0.64	0.492	0.586	1.15	1.08	0.834

The designs of both compressors are presented in FIGURE 15.

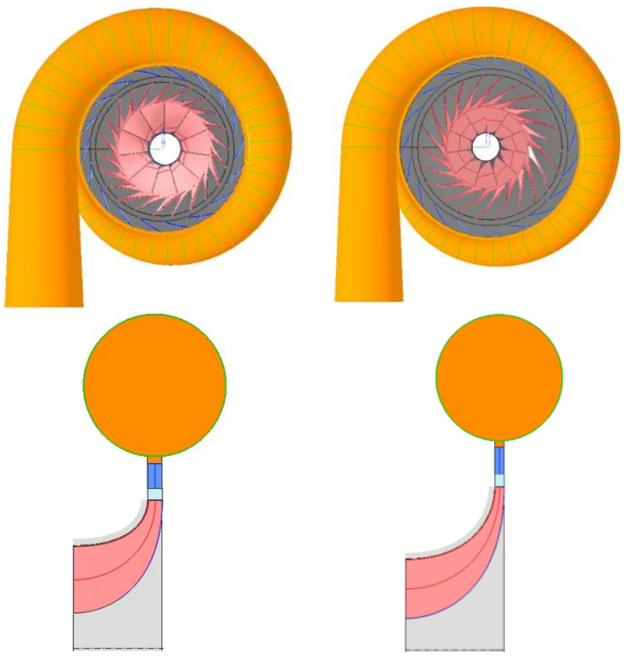

A) MFR=3.8 kg/s, D_{IMP} = 0.287 m B) MFR=20 kg/s D_{IMP} = 0.801 m

FIGURE 15: CENTRIFUGAL COMPRESSOR OPTIMAL SOLUTION

4. CONCLUSION

The presented materials confirm the applicability of the algorithms and methodologies, which were previously developed for axial compressors for the creation of accurate AI models to predict the geometry and performance of centrifugal compressors in a wide range of operational applications accompanied by the description and discussion of the peculiarities of technology application to a different compressor type.

The utilized approach allows for getting highly accurate models for flow path geometry and performance prediction of centrifugal compressors of various configurations, layouts, and designs that had not been achieved by the other authors who attempted to leverage NNs for centrifugal compressors. The accuracy level on the validation set for the geometry model is 99.7% and 99.6% for the performance model with an error threshold of 5%.

The created models were used in a cycle simulation environment to predict the most efficient combination of design variables of centrifugal compressors and avoid the need to pass the compressor design task to the compressor team during the system analysis step. Thus, eliminating the need for time-consuming and expensive iterations between cycle analysis and compressor design teams.

The developed technology provides the solid foundation for the development of AI models for other turbomachinery types as well as other components of gas turbine engines, power plants, refrigeration units, and other types of systems.

ACKNOWLEDGEMENTS

We wish to thank the many people from the SoftInWay, Inc. team who generously contributed their time and effort in the preparation of this work.

REFERENCES

[1] Balje, O. E. "A contribution to the problem of designing radial turbomachines." ASME Trans., 74, p. 451. 1952

[2] Moroz, Leonid. Govoruschenko, Yuri. and Pagur, Petr. "A Uniform Approach to Conceptual Design of Axial Turbine / Compressor Flow Path" Proceedings of the Future of Gas Turbine Technology 3rd International Conference (2006): Brussels, Belgium, October 2006

[3] K.V. Muralidharan. "Design of a Centrifugal Compressor Using CFD Analysis. Part I Preliminary Design and Geometry Modification." Proceedings of the ASME International Mechanical Engineering Congress and Exposition, 2014, Vol. 1, 2015

[4] G.L. Converse and R.G. Giffin. "Extended Parametric Representation of Compressors Fans and Turbines." Vol. I - CMGEN User's Manual. Technical Report No. NASA-CR-174645, General Electric Company, Cincinnati, Ohio. 1984

[5] S. ShashaVali, Ch. N. Chakravarthy, N. Prabhakar. "Modelling and analysis of centrifugal compressor 3D impeller." AIP Conf. Proc. 2358, 050009 (2021). DOI: 10.1063/5.005809

[6] Dehner R., Selamet A. "Three-Dimensional Computational Fluid Dynamics Prediction of Turbocharger Centrifugal Compression System Instabilities." Journal of Turbomachinery. August 2019, Vol. 141. 2019

[7] Hongsheng, Jiang. Dong, Sujun. Zheng, Liu. Yue, He. and Fengming, Ai. "Performance Prediction of the Centrifugal Compressor Based on a Limited Number of Sample Data." Mathematical Problems in Engineering Vol. 2019 (2019): Article ID 5954128, DOI 10.1155/2019/5954128

[8] Gholamrezaei, Mohammad. and Ghorbanian, Kaveh. "Compressor Map Generation Using a Feed-Forward Neural Network and Rig Data." Proceedings of the Institution of Mechanical Engineers Part A Journal of Power and Energy 224(1): pp. 97-108. Tehran, Iran, February, 2010. DOI: 10.1243/09576509JPE792

[9] Fei, Jingzhou. Zhao, Ningbo. Shi, Yong. Feng, Yongming. and Wang, Zhongwei. “Compressor Performance Prediction Using a Novel Feed-forward Neural Network Based on Gaussian Kernel.” Advances in Mechanical Engineering Vol. 8 (2016): DOI: 10.1177/1687814016628396

[10] Zhong, L. Liu, R. Miao, X. Chen, Y. Li, S. and Ji, H. “Compressor Performance Prediction Based on the Interpolation Method and Support Vector Machine.” Aerospace 2023, 10, 558. https://doi.org/10.3390/aerospace10060558

[11] Lorys, S.M. Orkisz, M. “Neural network approach to compressor modeling with surge margin consideration.” Archives of thermodynamics: Vol. 43(2022), No. 1, 89–108 DOI: 10.24425/ather.2022.140926

[12] Babu, C. J. Samuel, M.P. Davis, A. and Mishra, R. K. “Prediction of compressor nominal characteristics of a turboprop engine using artificial neural networks for build standard assessment.” International Journal of Turbo & Jet-Engines, DOI: 10.1515/tjj-2020-0015

[13] Massoudi, S., Picard, C. and Schiffmann, J. “Robust design using multiobjective optimization and artificial neural networks with application to a heat pump radial compressor.” Design Science, Volume 8, 2022, e1. DOI: https://doi.org/10.1017/dsj.2021.25

[14] Burlaka, Maksym. Podlech, Sascha. Moroz, Leonid. “Axial Compressor Map Generation Leveraging Autonomous Self-Training Artificial Intelligence. Phase 2” J. Eng. Gas Turbines and Power. September 2023: https://doi.org/10.1115/GT2023-102054

[15] Aungier, Ronald. “Axial–Flow Compressors: A Strategy for Aerodynamic Design and Analysis.” ASME International, New York (2003): pp. 361. ISBN 0-7918-0192-6.

[16] Ziegler, K. U. Gallus,H. E. and Niehuis, R. “A study on impeller-diffuser interaction: Part 1 - Influence on the performance.” GT-2002-30381. June 3-6. 2002

[17] Garret by Honeywell. Turbocharger Guide. Volume 4. p. 54.

[18] Sobol, Ilya. “On the distribution of points in a cube and approximate evaluation of integrals.” U.S.S.R Computational Mathematics and Mathematical Physics Vol. 7 No. 4 (1967): pp. 86–112. DOI: 10.1016/0041-5553(67)90144-9

[19] Catmull, Edwin; Rom, Raphael (1974). "A class of local interpolating splines". In Barnhill, Robert E.; Riesenfeld, Richard F. (eds.). Computer-Aided Geometric Design. pp. 317–326. doi:10.1016/B978-0-12-079050-0.50020-5. ISBN 978-0-12-079050-0.

[20] Wolfram Research (13 September 1996). Mathematica ® 3.0 Standard Add-on Packages. Cambridge University Press. ISBN 9780521585859.

[21] Levenberg, Kenneth (1944). "A Method for the Solution of Certain Non-Linear Problems in Least Squares". Quarterly of Applied Mathematics. 2 (2): 164–168. doi:10.1090/qam/10666

[22] Qingquan Song, Haifeng Jin, Xia Hu, Automated Machine Learning in Action, March 2022 ISBN 9781617298059 336 pages

[23] Github.com. “AutoKeras greedy tuner.” Available:https://github.com/keras-team/autokeras/blob/master/autokeras/tuners/greedy.py

[24] Kingma, Diederik. and Lei Ba, Jimmy. “Adam: A Method For Stochastic Optimization.” Proceedings of the 3rd International Conference for Learning Representations, San Diego, 2015

[25] Scikit-learn.org. “Standard Scaler.” Available: https://scikit-learn.org/stable/modules/generated/sklearn.preprocessing.StandardScaler.html

[26] TensorFlow.org. “Categorical Crossentropy.” Available: https://www.tensorflow.org/api_docs/python/tf/keras/losses/CategoricalCrossentropy

[27] Harris, David and Harris, Sarah (2012-08-07). Digital design and computer architecture (2nd ed.). San Francisco, Calif.: Morgan Kaufmann. p. 129. ISBN 978-0-12-394424-5.

[28] Storn, R.; Price, K. "Differential evolution - a simple and efficient heuristic for global optimization over continuous spaces". Journal of Global Optimization. 11 (4): 341–359, 1997. doi:10.1023/A:1008202821328

[29] Burlaka, Maksym. Moroz, Leonid. “Axial Compressor Map Generation Leveraging Autonomous Self-Training Artificial Intelligence” J. Eng. Gas Turbines and Power. Jan 2023, 145(1): 011001 (11 pages): DOI 10.1115/1.4055633

